BASIC PROPERTIES OF STARS

2.1   Introduction

Figure 2.1: Left: *Hubble Space Telescope* image of the star cluster NGC 265 in the Small Magellanic Cloud. Right: ESO *Very Large Telescope* image of the cluster Trumpler 14 in the Carina nebula. This ground-based image has been sharpened with Adaptive Optics techniques.

Figure 2.1 shows two examples of star clusters. Star clusters allow us to appreciate directly some of the physical properties of stars for the simple reasons that, to a first approximation, all the stars of a cluster: (i) are at the same distance from the Sun, and (ii) have the same age. NGC 265 (left panel of Figure 2.1) is approximately 300 million years old and is located in the Small Magellanic Cloud, one of our two companion galaxies at a distance of ~ 60 kpc. Trumpler 14 (right panel of Figure 2.1) is one of the youngest stellar clusters known, with an age of only 1 million years. It is associated with the Carina nebula at a distance of 3.2 kpc.

It is immediately obvious from these images that: (a) stars have a range of colours, and (b) some stars are intrinsically brighter than others. More generally, we can make a list of what we may consider to be the most important physical properties of a star:

1. **Mass**

2. Temperature

3. Luminosity

4. Gravity

5. Age

6. Chemical Composition

These parameters are all inter-related but, to a first approximation, it is the first one, the mass of a star, that determines its temperature, luminosity, surface gravity and lifetime. The chemical composition is only a second order effect. In this lecture, we'll consider how some of these properties are determined. However, before we can measure the intrinsic characteristics of a star, we need to establish its distance.

2.2 Stellar Distances

We have already encountered the stellar parallax in Lecture 1. Referring to Figure 1.3, with $R = 1\,\mathrm{AU}$, we have:

$$\frac{R}{d} = \tan\theta \simeq \sin\theta \simeq \theta \tag{2.1}$$

for small angles θ, and therefore

$$d = \frac{R}{\theta}. \tag{2.2}$$

By definition, $d = 1\,\mathrm{pc}$ when $\theta = 1\,\mathrm{arcsec}$.

Note that the nearest star, Proxima Centauri, is at a distance $d = 1.3\,\mathrm{pc}$, corresponding to $\theta = 0.764\,\mathrm{arcsec}$, comparable to the size of a stellar image as measured from the ground through the turbulence introduced by the Earth's atmosphere. For this and other complicating reasons, $\theta \gtrsim 0.01\,\mathrm{arcsec}$, $d \lesssim 100\,\mathrm{pc}$ is the limit of parallax measurements from the ground.

The *Hipparcos* satellite, a European Space Agency (ESA) Space Astrometry Mission launched in 1989, successfully observed the celestial sphere for 3.5 years and measured the positions (Right Ascension and Declination) and parallax of over $100\,000$ stars within $d \lesssim 1000\,\mathrm{pc}$ ($\theta \gtrsim 0.001\,\mathrm{arcsec}$).

When completed, the current ESA Space Astrometry Mission, *Gaia*, launched in December 2013, will be a major leap forward:

- Positional accuracy: from $0.001\,\mathrm{arcsec}$ to $0.00001\,\mathrm{arcsec}$ ($\times 10^2$)

- Distance: from $1\,\mathrm{kpc}$ to $100\,\mathrm{kpc}$, sufficient to reach stars in neighbouring galaxies!

- Sensitivity: from 10 mag to 20 mag ($\times 10^4$)

- Number of stars: from 10^5 to 10^9 ($\times 10^4$)

Note 1: By combining the parallactic distance with the angular position on the sky (RA and Declination), we have the location of a star in 3-D.

Note 2: Parallactic stellar distances are the first rung of the 'cosmic distance ladder'. Consider two stars, with observed magnitudes m_1 and m_2 respectively, such that $m_2 > m_1$ (i.e. star 2 is fainter than star 1). Consider the case where star 1 has a parallactic distance, but star 2 is too far away to give a measurable parallax. If we have reasons to believe that the two stars have the same *absolute magnitude*, we can derive a *photometric distance* for star 2 using the inverse square behaviour of stellar fluxes, F:

$$\frac{F_2}{F_1} = 10^{0.4 \times (m_1 - m_2)} = \left(\frac{d_1}{d_2}\right)^2 \tag{2.3}$$

using the relation between stellar fluxes and magnitudes given in Lecture 1, so that

$$d_2 = d_1 \times 10^{-0.4 \times (m_1 - m_2)/2} \tag{2.4}$$

The above equations assume that the dimming of star 2 relative to star 1 is due entirely to its greater distance and neglects other possible sources of dimming, such as interstellar extinction by dust. This is the method used

to derive distances on cosmological scales; it relies on establishing a series of 'standard candles', by which astronomers mean astronomical sources of known absolute magnitude, at increasing distances to build a cosmological distance ladder.
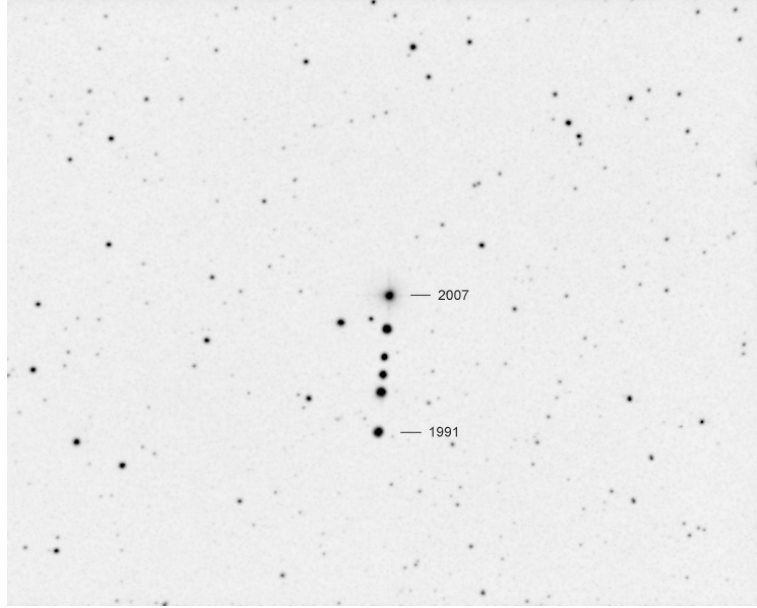
2.2.1 Proper Motion

Figure 2.2: Proper motion of Barnard's star. This low-mass red dwarf is the fourth closest star to the Sun after the three components of the α Cen system, at a distance of 1.83 pc ($\theta = 0.545$ arcsec), and has the highest measured proper motion, $\mu = 10.4$ arcsec yr^{-1}.

If we measure the celestial coordinates (RA and Dec) of a nearby star at the same time each year (or in practice if we correct for the effects of the Earth's orbit around the Sun), we find that its position in a reference frame based on very distant objects such as quasars is not the same from year to year (see Figure 2.2). This is *proper motion*, reflecting the fact that the positions of stars within the Galaxy are not fixed. For example, the whole Galactic disk rotates with a circular velocity $v_{\rm rot} = 220$ km s^{-1} at the Sun's position. Superposed on this regular rotation pattern is a random velocity of individual stars with dispersion $\sigma_{\rm disk} \simeq 20$ km s^{-1} in the direction perpendicular to the Galactic plane. Stars in the Milky Way halo have much higher random motions: $\sigma_{\rm halo} \simeq 100$ km s^{-1}; when one of these stars intersects the Galactic plane near the Sun's location its proper motion can substantial.

Note 1: Proper motions are measured in arcsec yr^{-1}; values for all but the nearest stars are $\mu \ll 1\,\mathrm{arcsec\ yr}^{-1}$.

Note 2: What we measure as proper motion is the component of the star's motion *perpendicular* to the line of sight from the Sun to the star. Proper motions are generally quoted separately in RA and Dec.

Note 3: If we know the distance to a star, then we can deduce its transverse velocity (in km s^{-1}) from its proper motion.

2.2.2   Doppler Shift and Space Motion

By now you should be familiar with the concept of redshift, the shift to longer wavelengths (perceived as red by the human eye) of light waves as a result of the relative motions (apart) of emitter and receiver. A few points of note:

- In astronomy, in order to measure redshifts, we need to record the spectra of astronomical sources and measure the wavelength(s) of well-defined spectral feature(s), such as emission or absorption lines. Colours are not sufficient because stars and galaxies can appear red because they are cool, or because their light is reddened by interstellar dust.

- When we are dealing with nearby objects, we measure a Doppler (kinematic) redshift or blueshift:

$$z = \frac{\lambda_{\mathrm{obs}} - \lambda_0}{\lambda_0} \tag{2.5}$$

  where λ_{obs} is the observed wavelength of a given spectral line, and λ_0 is the rest-frame wavelength of the same atomic transition, as measured in the laboratory.

- With the Doppler redshift/blueshift is associated a *radial velocity*

$$v = c \cdot z \tag{2.6}$$

  where v is positive for objects moving away from us and negative for objects approaching us.

- Eq. 2.6 is the limiting case (for $v \ll c$) of the special relativity result

$$1 + z = \sqrt{\frac{1 + v/c}{1 - v/c}} \qquad (2.7)$$

For stars with measured parallaxes and proper motions, the combination of transverse and radial velocity measurements gives the full space velocity of the stars in 3D (see Figure 2.3).
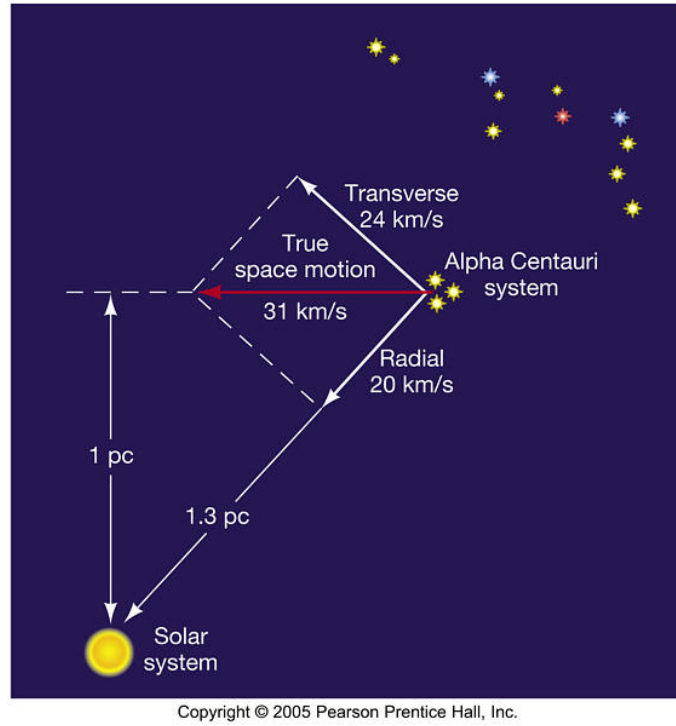
Figure 2.3: By combining proper motion with radial velocity measurements, it is possible to deduce the true space motion of a celestial object.

The velocities and positions of such stars within the Galaxy are fully specified by the six parameters:

l = Galactic longitude (degrees),
b = Galactic latitude (degrees),
d = distance (kpc) from the Galactic Centre,
U = radial velocity relative to the Galactic centre (+ve towards the Galactic centre) ,
V = velocity around the axis of Galactic rotation (+ve in the direction of Galactic rotation), and
W = velocity parallel to the axis of Galactic rotation (+ve in the direction of North Galactic pole).

All six vectors are only available for a relatively small number of stars, because while it is relatively easy to measure celestial coordinates and radial velocities with the necessary accuracy, distances and proper motions are available only for nearby stars. Great improvements expected from the *Gaia* mission which has been designed to measure all six parameters (plus other properties) for one billion stars (still only 1% of the Galactic stellar population!).

2.3   Magnitudes and Luminosities

We have already introduced these concepts in Lecture 1. Magnitudes and luminosities are normally measured through a given filter; Figures 2.4 and 2.5 show the transmission curves of some of the most commonly used optical and near-infrared filters. Note that the near-IR filters are designed to approximately match the transmission windows of the atmosphere at these wavelengths.

It can be appreciated from the Figures that this is hardly a desirable state of affairs. Ideally, we would like the filter transmission curves to be rectangular: 100% transmission over the desired range of wavelengths and 0% everywhere else. Instead, there are ripples and broad tails. There are also pronounced differences between different filter sets, with the potential for error when converting from one set of magnitudes to another.
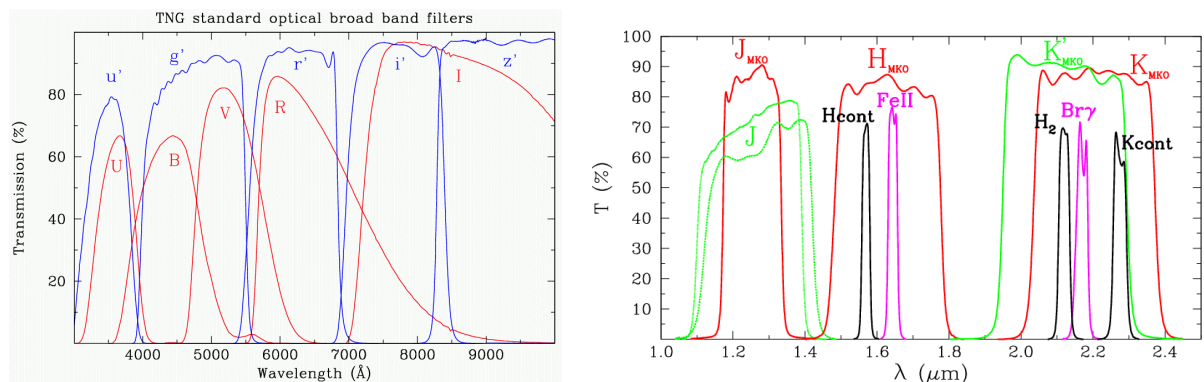

Figure 2.4: Left: Transmission curves of the most commonly used optical broad-band filters. The red curves are for filters in the Johnson-Cousins system, while the blue curves are for the Gunn filters used by the Sloan Digital Sky Survey (SDSS). Right: Transmission curves for commonly used near-IR filters. The narrow-band filters isolate spectral features of particular interest.
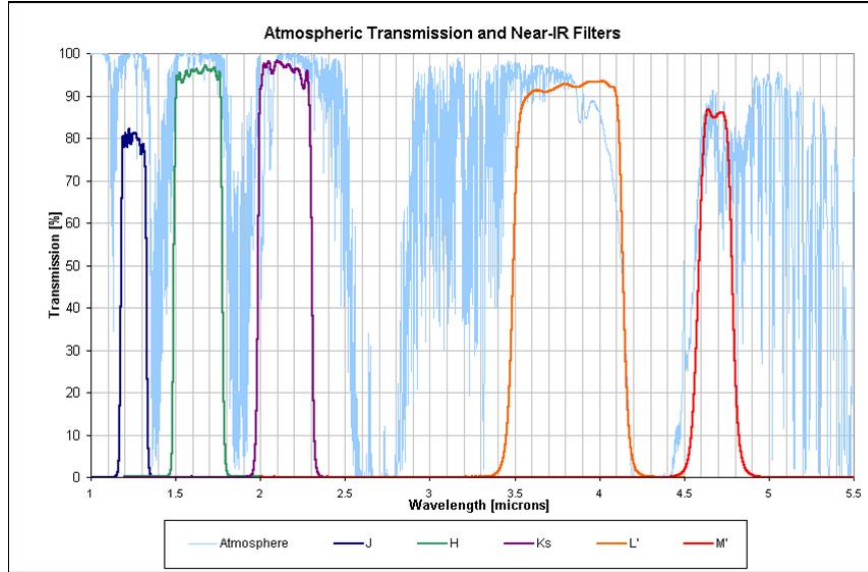
Figure 2.5: Near-IR atmospheric transmission curves and filters.

To circumvent some of these problems, the monochromatic AB magnitude system was defined as:

$$AB = -2.5 \log_{10} f_\nu - 48.60 \tag{2.8}$$

where f_ν is the flux density measured in ergs s^{-1} cm^{-2} Hz^{-1}. AB magnitudes are used mostly in extragalactic astronomy.

The star α Lyrae provides the zero point of broad-band magnitude systems, since by definition it has $m = 0.00$ in all bands. Again, this is not ideal when one considers that the flux emitted by α Lyrae per unit wavelength (or frequency) interval is far from constant with wavelength (see Figure 2.6).

Some illustrative magnitudes:

Table 2.1 Apparent and absolute magnitudes of selected astronomical sources

| Object	Apparent mag m_V	Absolute mag M_V
Sun	−26.7	+4.8
α Canis Majoris (Sirius, brightest star)	−1.4	+1.42
α Lyrae (Vega)	0.0	+0.58
ζ Orionis (in Orion's belt)	+2.0	−5.3
Faintest star visible from Cambridge street	+3.5	
Faintest star visible from dark site, dark adapted	+6.0	
R136 (brightest stellar cluster in LMC)	+9.5	−8.9
Type II Supernova in nearby galaxy	$\sim$ +14	−15.3
QSO 3C273 (first known quasar)	+12.9	−26.5
Faintest galaxy in the Hubble Ultra-Deep Field	$\sim$ +30	
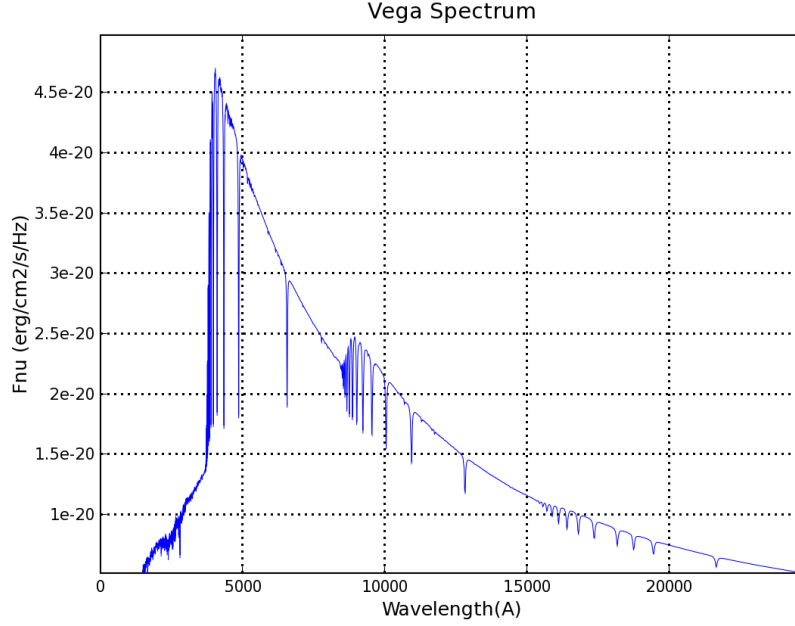
Figure 2.6: The spectrum of α Lyrae, from the near-UV to the near-IR.

Magnitudes can be measured very precisely (to ~ 0.1 millimags from space with the *Kepler* mission), to the extent that it is now possible to infer the existence of Earth-size exoplanets from the shadowing of the stellar disk caused by the planet transiting in front of a solar-type star.

2.4 Effective Temperatures of Stars

The temperature in the interior of stars can reach several 10^8 K. However, of interest here is the *effective temperature*, T_{eff}, of the visible outer layers which radiate the light we see and record with our telescopes. The term *effective temperature* refers to the temperature of a blackbody that most closely approximates the emergent spectrum of a star (see Figure 2.7 left). The continuum spectrum of a blackbody is described by the Planck function (see Figure 2.7 right):

$$B_\lambda(T) \text{ [erg s}^{-1} \text{ cm}^{-2} \text{ Å}^{-1} \text{ sr}^{-1}] = \frac{2hc^2/\lambda^5}{e^{hc/\lambda kT} - 1} \qquad (2.9)$$

$$B_\nu(T) \text{ [erg s}^{-1} \text{ cm}^{-2} \text{ Hz}^{-1} \text{ sr}^{-1}] = \frac{2h\nu^3/c^2}{e^{h\nu/kT} - 1} \qquad (2.10)$$

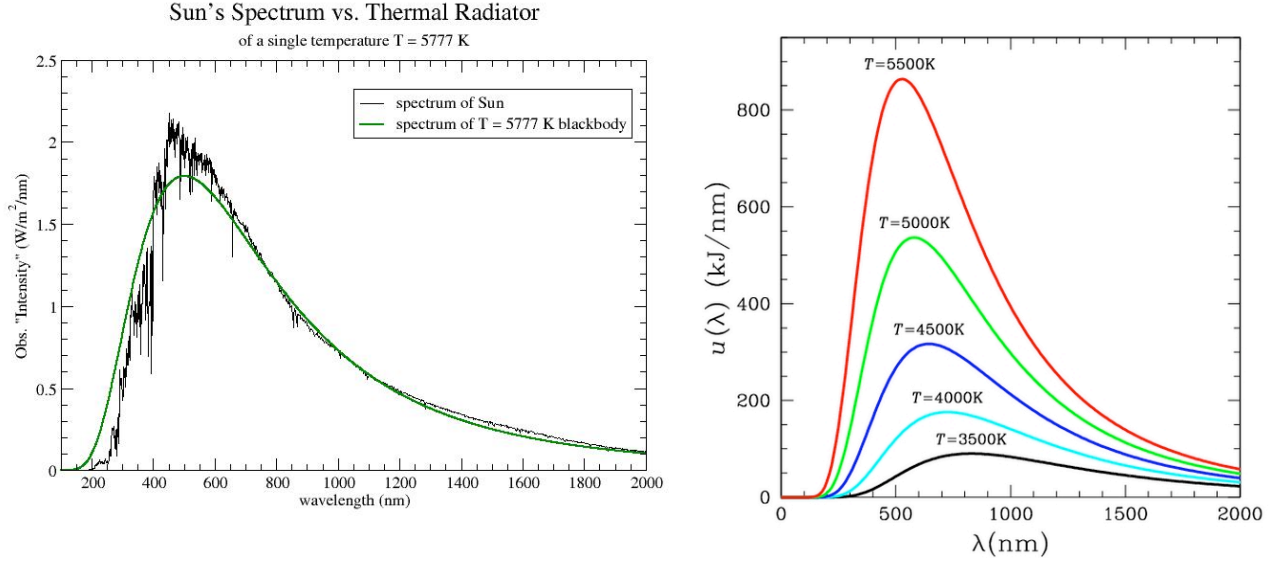Note two important properties of the spectrum described by eq. 2.9:

Figure 2.7: Left: The light output from the Sun at visible wavelengths can be approximated by a blackbody spectrum with $T = 5777\,\text{K}$. Right: Blackbody curves for different temperatures.

(1) By considering $dB_\lambda/d\lambda = 0$ to determine the maximum of the function B_λ, we find that

$$\lambda_{\max} T = 0.290\,\text{cm K} \tag{2.11}$$

which is known as Wien's displacement law. For a star like the Sun, with $T_{\text{eff}} = 5770\,\text{K}$, $\lambda_{\max} = 5020\,\text{Å}$.

(2) Figure 2.7 (right) also shows that as its temperature increases, a blackbody emits more energy per second at *all* wavelengths. Integrating eq. 2.9 we find:

$$\int B_\lambda(T)d\lambda = \frac{\sigma}{\pi}T^4 \tag{2.12}$$

where σ is the Stefan-Boltzmann constant ($\sigma = 5.67\times10^{-5}\,\text{erg s}^{-1}\,\text{cm}^{-2}\,\text{K}^{-4}$).

To obtain the total luminosity of a blackbody, we multiply by its surface area and integrate over the solid angle:

$$L = 4\pi R^2 \times \int B_\lambda(T)d\lambda \cdot \int d\Omega \tag{2.13}$$

$$L = 4\pi R^2 \times \int B_\lambda(T)d\lambda \cdot \int_0^{2\pi} d\phi \int_0^{\pi/2} \cos\theta \sin\theta d\theta \tag{2.14}$$

$$L = 4\pi R^2 \frac{\sigma}{\pi}T^4 \pi \;=\; 4\pi R^2 \sigma T^4 \tag{2.15}$$

Eqs. 2.11 and 2.15 are very powerful. Eq. 2.11 tells us that, if we measure the magnitude of a star through two filters (see Figure 2.4), we can immediately deduce its T_{eff} since, for example:

$$m_B = -2.5 \log F_B + \text{const}$$

$$m_V = -2.5 \log F_V + \text{const}$$

so that:

$$B - V = -2.5 \log(F_B/F_V)$$

where F is the flux through the appropriate filter. Comparison of the measured $B-V$ *colour* with those of blackbodies of different temperatures then yields a photometric estimate of T_{eff}.

We now have an interpretation for the different colours of stars (e.g. Figure 2.1): *they reflect the fact that stars have different temperatures.* Here are some examples:

Table 2.2 $B-V$ colours and effective temperatures
of some nearby stars

Object	$B-V^{\dagger}$ (mag)	T_{eff} (K)
HD 14434	-0.33	47 000
ζ Oph	-0.31	34 000
τ Sco	-0.30	30 000
α Lyr	0.00	9790
51 Aql	$+0.30$	7300
Sun	$+0.63$	5777
31 Ori	$+1.50$	4050
19 Ari	$+1.56$	3690
α Ori	$+1.71$	3370
Wolf 359	$+2.03$	2800

† Corrected for interstellar reddening

Astronomers use the term 'colour' or 'colour index' to refer to the difference in magnitude between any two filters (see Figure 2.4). Conventionally, colours are specified in the sense (shorter wavelength)−(longer wavelength). Thus we have $U - B$, $B - V$, $V - R$, $V - K$, and so on.

Returning to eq. 2.15, we can see that a star's luminosity depends on both its temperature and size. With a knowledge of a star's T_{eff} (from its colour)
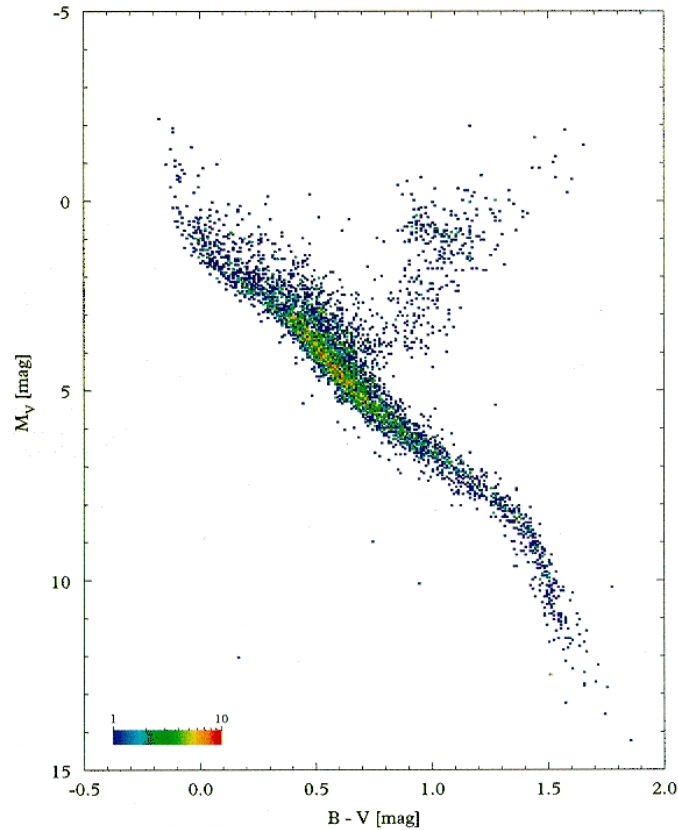
Figure 2.8: H-R diagram for nearby stars with measured parallaxes from the Hipparcos mission.

and luminosity (from its measured magnitude and distance), we can obtain an estimate of its radius.[1]

For stars at known distances (or for stars all at the same distance within a cluster), we can construct a diagram plotting their luminosity as a function of colour, as in Figure 2.8. This is undoubtedly the most import diagram in stellar astronomy and we shall explore it in detail during the course of these lectures. It is referred to as the Hertzsprung–Russell diagram (HRD) from the names of the astronomers who first constructed it in the 1910s, or more generally as a colour-magnitude diagram.

We can immediately make the following observations:

- Most of the stars are found in relatively narrow strip on the $M_V - (B - V)$ plane. This strip is the *Main Sequence.*

- Stars of the same $(B - V)$ colour, or equivalently of the same T_{eff}, can

---

[1]The radii of the nearest stars have been measured directly via optical interferometry; these measure generally agree with the values deduced assuming that the stars radiate as blackbodies.
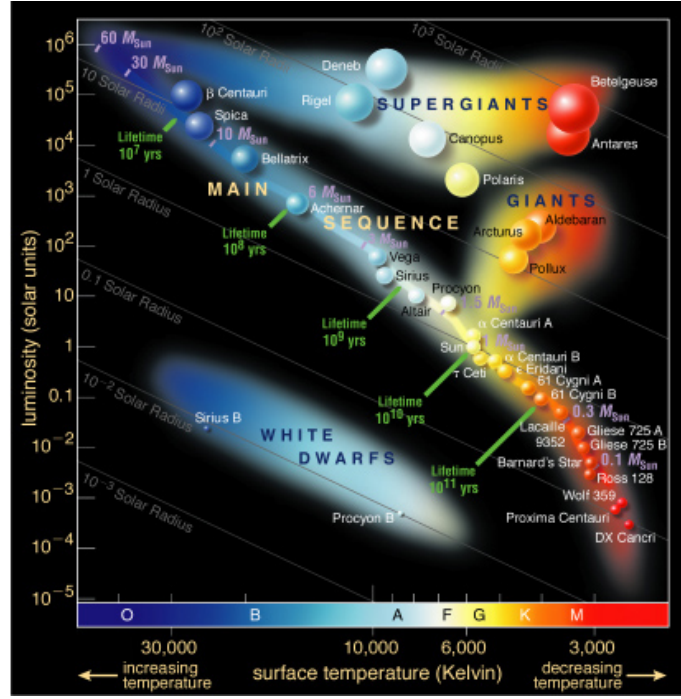
Figure 2.9: Locations of some bright stars on the H-R diagram.

have widely different luminosities. For example, stars with $(B - V) \simeq$ 1.0 in Figure 2.8 have values of M_V which span 10 magnitudes, or a factor of 10 000! From eq. 2.15 we understand this to be a consequence of their different sizes; evidently, the radii of such stars span a range of two orders of magnitude. For this reason, stars above the main sequence are termed *giants* and *supergiants*, while stars below the main sequence are *sub-dwarfs*.

- Although the stars collected in Figure 2.8 do not constitute a volume-limited sample (that is, Hipparcos did not measure all the stars within a given distance from the Sun), it is still evident that only a few stars are located away from the Main Sequence. The most straightforward interpretation of this observation is that stars must spend most of their life on the Main Sequence. Thus, the H-R diagram charts stellar evolution: stars move onto the Main Sequence when they are born and evolve off the Main Sequence during the late stages in their evolution.